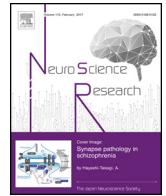




Contents lists available at [ScienceDirect](#)

Neuroscience Research

journal homepage: www.elsevier.com/locate/neures



6-Deoxyjacareubin, a natural compound preventing hypoxia-induced cell death, ameliorates neurodegeneration in a mouse model of familial amyotrophic lateral sclerosis

Tomonori Hoshino, Shu-ichi Matsuzawa*, Ryosuke Takahashi*

Department of Neurology, Graduate School of Medicine, Kyoto University, Kyoto, 606-8507, Japan

ARTICLE INFO

Article history:

Received 2 December 2019
Received in revised form 4 February 2020
Accepted 25 February 2020
Available online xxx

Keywords:

Amyotrophic lateral sclerosis
Cell death
Cu/Zn superoxide dismutase
6-Deoxyjacareubin
Hypoxia
Neurodegeneration

ABSTRACT

The central nervous system (CNS) uses a significant amount of oxygen for energy production. Decreased oxygen supply due to impaired blood supply critically damages the CNS. As chronic hypoxic conditions have diverse effects via the excessive production of reactive oxygen species, protection from hypoxic damage is important for cell survival. Recent studies have revealed that various markers of hypoxia are altered in age-related neurodegenerative diseases such as amyotrophic lateral sclerosis (ALS), indicating the involvement of hypoxia. However, therapeutic strategies targeting hypoxia-induced pathways in ALS have not been developed yet. We previously screened small-molecule compounds that inhibit hypoxia-induced cell death and identified 6-deoxyjacareubin. We hypothesized that the modulation of hypoxia signaling by 6-deoxyjacareubin might protect motor neurons in ALS. Here, we show that 6-deoxyjacareubin indeed ameliorates neurodegeneration in a mouse model of familial ALS. Administration of 6-deoxyjacareubin to this familial ALS model significantly attenuated disease progression and improved locomotor dysfunction. We also found that 6-deoxyjacareubin reduced motor neuron loss and glial activation. Our results indicate that 6-deoxyjacareubin might serve as a potential therapeutic tool for ALS. Moreover, these results suggest that modulation of hypoxia signaling pathways provides a promising strategy to develop therapies for other types of neurodegenerative diseases also characterized by hypoxia.

© 2020 Elsevier B.V. and Japan Neuroscience Society. All rights reserved.

1. Introduction

Amyotrophic lateral sclerosis (ALS), also known as Lou Gehrig's disease or motor neuron disease, is an adult-onset neurodegenerative disease characterized by loss of upper and lower motor neurons in the spinal cord and motor cortex (Brown and Al-Chalabi, 2017; van Es et al. (2017v)). Patients with ALS show progressive muscle weakness and atrophy, and the disease finally causes lethal respiratory failure within 3–5 years of onset. Although ~10% of ALS cases are familial, the majority of cases are sporadic. Whereas extensive studies have identified several familial ALS genes, there is currently no effective treatment to halt the progression of ALS. Superoxide dismutase 1 (SOD1) is the first gene to be identified in which

mutations are associated with familial ALS cases and accounts for ~12–20% of familial ALS cases (Renton et al., 2014; Rosen et al., 1993; Taylor et al., 2016). Because rodent strains carrying a human SOD1 mutation such as SOD1^{G93A} show an ALS-like phenotype characterized by progressive locomotor dysfunction, motor neuron loss, and activation of microglia and astrocytes, these models have been used widely as familial ALS models (Philips and Rothstein, 2015).

The central nervous system (CNS) requires significant amounts of oxygen for adenosine triphosphate (ATP) production (Girouard and Iadecola, 2006; Zlokovic, 2008). Once oxygen supply is compromised due to impaired blood supply, the CNS is critically damaged. Using a mouse model of familial ALS, one study revealed that the neurovascular unit is disrupted prior to motor neuron degeneration and that spinal blood flow is impaired at presymptomatic stages, indicating relative hypoxia in motor neurons (Miyazaki et al., 2012, 2011). Furthermore, intermittent hypoxia aggravates motor neuron loss in a mouse familial ALS model (Kim et al., 2013). Sustained hypoxia has a number of consequences including cell death and inflammation by inducing excessive production of reactive oxygen

Abbreviations: ALS, amyotrophic lateral sclerosis; ROS, reactive oxygen species; SOD1, Cu/Zn superoxide dismutase; 6-Deox, 6-Deoxyjacareubin.

* Corresponding authors at: 54 Shogoin-Kawahara-cho, Sakyo-ku, Kyoto, 606-8507, Japan.

E-mail addresses: smatsuz@kuhp.kyoto-u.ac.jp (S. Matsuzawa), ryosuket@kuhp.kyoto-u.ac.jp (R. Takahashi).

<https://doi.org/10.1016/j.neures.2020.02.011>

0168-0102/© 2020 Elsevier B.V. and Japan Neuroscience Society. All rights reserved.

species (ROS) (Tafari et al., 2016). In fact, accumulation of oxidative stress markers is observed in rodent models of ALS, as well as in patients with ALS (Barber et al., 2006; Casoni et al., 2005; Chang et al., 2008; Niedzielska et al., 2016). Cells adapt to changes caused by increased hypoxic stress by upregulating pathways related to antioxidation (e.g., heme oxygenase 1, HO-1), angiogenesis (e.g., vascular endothelial growth factor, VEGF), or glycolysis (e.g., hexokinase 2, HK2) via stabilizing hypoxia-inducible factor 1 alpha (HIF-1 α) (Cavadas et al., 2016; Iyer et al., 1998). Elevated levels of hypoxia-related products such as HIF-1 α are observed in both ALS rodent models and patients with ALS (Nagara et al., 2013; Sato et al., 2012). Considering that hypoxia is observed in other neurodegenerative diseases such as Alzheimer's disease and Parkinson's disease (Asllani et al., 2008; Foti et al., 2010; Gutiérrez-Jiménez et al., 2018; Iturria-Medina et al., 2016; Love and Miners, 2016; Nielsen et al., 2017; Nortley et al., 2019; Zeisel et al., 2018), these results implicate hypoxia in the pathogenesis of ALS and suggest that the modulation of hypoxia signaling pathways plays an important role in neurodegeneration. However, the effects of modulating these pathways in ALS remain unclear.

In previous assays, we screened small-molecule compounds against chemically induced hypoxia (cobalt chloride; CoCl₂) and sealed chamber hypoxia (0.5% O₂) by assessing cell viability, and we identified several compounds that protect against hypoxia-induced cell death (unpublished data). Furthermore, in a structure-activity relationship (SAR) study, we found that 6-deoxyjacareubin is a candidate compound. In addition, this compound has neuroprotective effects in an experimental rat model of glaucoma (unpublished data). 6-Deoxyjacareubin is a natural xanthone, initially isolated from the leaves of *Vismia latifolia* (Fig. 1A), and is used in traditional Brazilian medicine as a tonic and antipyretic agent (Doriguetto et al., 2001). This compound has been reported to have many biological properties, including anticancer (Teh et al., 2013), antifungal (Rocha et al., 1994), and antioxidant (Yi et al., 2011) functions, and inhibition of the platelet-activating factor receptor (PAFR) (Jantan et al., 2002; Oku et al., 2005). However, the beneficial effect of 6-deoxyjacareubin in neurodegenerative diseases such as ALS is unknown. We hypothesized that the modulation of hypoxia signaling by 6-deoxyjacareubin would protect compromised motor neurons in *in vivo* models of ALS. To assess its benefits in motor neuron disease, we treated ALS model mice with 6-deoxyjacareubin.

2. Materials and methods

2.1. Study design and reagents

The objective of this study was to investigate the efficacy of 6-deoxyjacareubin in inhibiting hypoxia-induced cell death in SOD1^{G93A} mice. All experiments were performed in accordance with approved guidelines. We purchased 6-deoxyjacareubin (CAS#16265-56-8) from ALB Technology Limited (Henderson, NV, USA) and Aldab Chemicals (Boston, MA, USA), CoCl₂•6H₂O (cat#C-8661) and Cremophor EL (cat#C5135) from Sigma-Aldrich (St. Louis, MO, USA), saline solution from Otsuka Pharmaceutical Factory (Tokushima, JPN, cat#2402187), dimethyl sulfoxide (DMSO; cat#09659-85) and hydrogen peroxide (H₂O₂; cat#18411-25) from Nacalai Tesque (Kyoto, JPN), isoflurane (cat#133403) from Pfizer (New York, NY, USA), erastin (cat#329600) from Calbiochem (San Diego, CA, USA), and staurosporine (cat#197-10251) from Wako (Osaka, JPN).

2.2. Cell culture

Human HEK293T cells (RRID: CVCL_0063, American Type Culture Collection; ATCC, Manassas, VA, USA) were cultured in

high glucose Dulbecco's Modified Eagle's Medium (DMEM; Wako, cat#043-30085) supplemented with 10% fetal bovine serum (FBS; Gibco, Grand Island, NY, USA, cat#10270) and 1% penicillin-streptomycin (PS) solution (Nacalai Tesque, cat#26253-84) in a humidified incubator with 5% CO₂ at 37 °C. For hypoxia treatment, the cells were incubated for 24 h under hypoxic conditions (1% O₂, 5% CO₂) using the Anaero Pack System for cells (Mitsubishi Gas Chemical, Tokyo, JPN, cat#1-8754-01). A maximum of seven cell passages was used.

2.3. Cell viability assay

HEK293T cells were seeded at 10,000 cells per well in 96-well plates coated with collagen (CellMatrix, Nitta-Gelatin, Osaka, JPN, cat#KP-4100) in DMEM supplemented with 1% FBS and 1% PS. Cell viability was measured using the CellTiter-Glo2 assay (Promega, Fitchburg, WI, USA, cat#G9242) or the Cell Count Reagent SF (WST-8 assay; Nacalai Tesque, cat#07553-44) according to the manufacturer's protocols. All plate assays were measured using an ARVO X5 (PerkinElmer, Waltham, MA, USA). n = 3 per group.

2.4. Mice

Male human SOD1^{G93A} transgenic mice (B6.Cg-Tg(SOD1*G93A)1Gur/J; SOD1^{G93A} mice, RRID: IMSR_JAX:004435) were obtained from the Jackson Laboratory (Bar Harbor, ME, USA). Male SOD1^{G93A} mice were bred with female C57BL/6J mice purchased from Charles River Japan, Inc. (Shiga, JPN). The mice were housed under standard conditions, i.e., at 24 °C \pm 2 °C, 50% \pm 10% humidity, and a 12-h light/dark cycle, with free access to food and water in a specific pathogen-free vivarium. For genotyping, we used the forward primer 5'-CTAGGCCACAGAATTGAAAGATCT-3' and the reverse primer 5'-GTAGGTGGAATTCTAGCATCATCC-3' to detect mouse-derived *Sod1* (IMR7338 and IMR7339) and used the forward primer 5'-CATCAGCCCTAATCCATCTGA-3' and the reverse primer 5'-CGCGACTAACAACTCAAAGTGA-3' to detect human-derived *SOD1* (IMR0113 and IMR0114). SOD1^{G93A} mice weighing more than 22 g (seven weeks old) were used for the treatment group. Age-matched littermates of end-stage (145–160 days) ALS mice were used for RT-qPCR analysis, Nissl staining, and immunohistochemistry.

All studies were performed in accordance with the Guidelines for Animal Studies of Kyoto University (MedKyo17589, MedKyo18224, and MedKyo19227).

2.5. RNA extraction and real-time quantitative polymerase chain reaction analysis

Total RNA was extracted using TriPure (Roche, Basel, CHE, cat#11667165001) and RNeasy mini plus kit (Qiagen, Germantown, MD, USA, #74136) according to the manufacturer's instructions with slight modification. Briefly, the spinal cord from mice was homogenized using a QIA shredder (Qiagen, cat#79656) in a TriPure isolation reagent. After adding chloroform, the sample was centrifuged at 12,000 \times g for 15 min at 4 °C. The upper aqueous phase was transferred to a gDNA eliminator spin column and centrifuged at 8,000 \times g for 30 s. After that, the same volume of 70% ethanol was added to the flow-through and applied to a RNeasy spin column. Total RNA was reconstituted in RNase free water. cDNA was synthesized from total RNA using PrimeScript RT Master Mix (Perfect Real Time; TaKaRa Bio Inc., Shiga, JPN, cat#RR036A). Real-time quantitative polymerase chain reaction (RT-qPCR) analysis was performed using a LightCycler 480 (Roche) with the LightCycler 480 SYBR Green I master mix (Roche, cat#04887352001). For all experiments, expression levels were normalized to those of glyceraldehyde-3-phosphate dehydrogenase (*Gapdh*). The primers

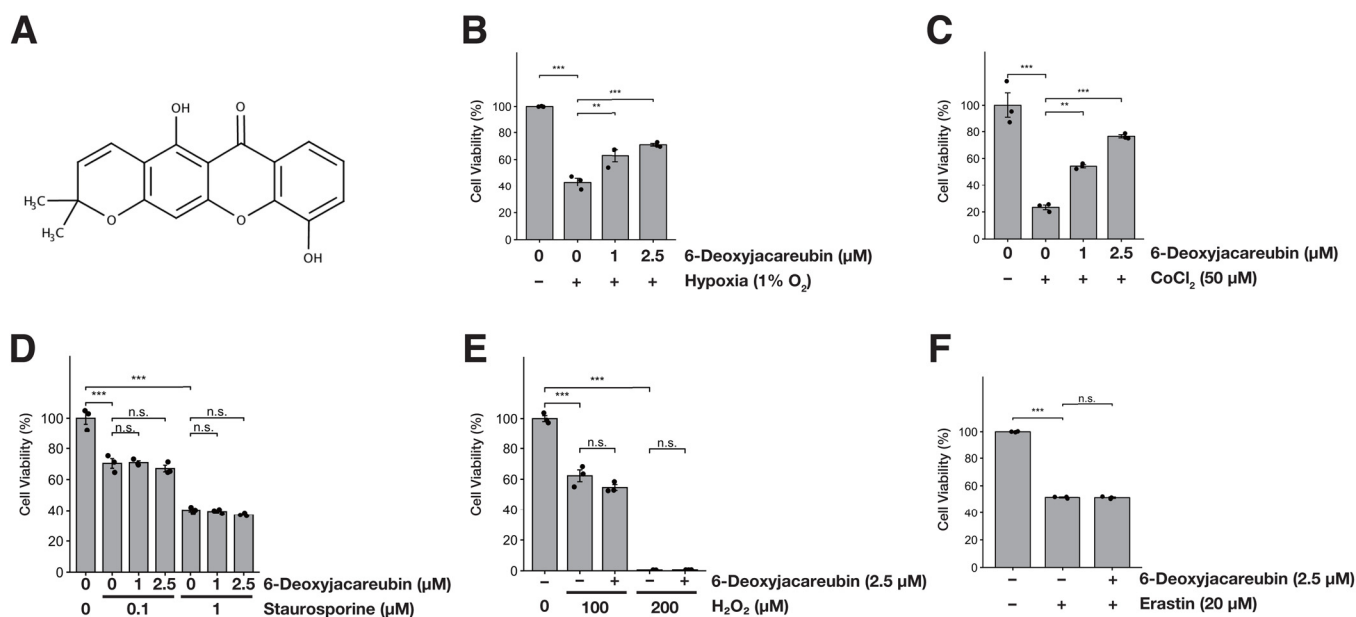


Fig. 1. 6-Deoxyjacareubin inhibits hypoxia-induced cell death via a non-apoptotic pathway. (A) Structure of 6-deoxyjacareubin. (B) HEK293T cells were treated with sealed chamber hypoxia (1 % O₂) in the presence or absence of 6-deoxyjacareubin. (C) HEK293T cells were treated with the chemical hypoxia-inducing agent CoCl₂ in the presence or absence of 6-deoxyjacareubin. (D) HEK293T cells were treated with the apoptosis-inducing agent staurosporine in the presence or absence of 6-deoxyjacareubin. (E) HEK293T cells were treated with H₂O₂ in the presence or absence of 6-deoxyjacareubin. (F) HEK293T cells were treated with the ferroptosis-inducing agent erastin in the presence or absence of 6-deoxyjacareubin. (B–F) Cell viability was measured using the CellTiter-Glo2 assay. n = 3 per group. Data are presented as the mean ± SEM normalized to the control group. **: p < 0.01. ***: p < 0.001. n.s.: not significant. One-way ANOVA followed by Tukey's post hoc test.

used for this study are listed in the Supplementary Table. n = 3–4 per group.

2.6. Administration of 6-deoxyjacareubin, onset time, and survival

For administration of 6-deoxyjacareubin, the mice were randomly divided into three groups: wild-type (WT) + vehicle group; SOD1^{G93A} + vehicle group; SOD1^{G93A} + 6-deoxyjacareubin. No blinding was performed in this study. Starting at the age of eight weeks, male SOD1^{G93A} mice were injected intraperitoneally (i.p.) with 100 μL of 6-deoxyjacareubin (5 mg kg⁻¹) or vehicle (10 % DMSO and 10 % Cremophor EL in saline) every seven days for 1 month. Disease onset was determined as the time when the mice reached the maximum weight (Endo et al., 2015). Mice were considered to have reached end-stage disease when they were unable to right themselves within 20 s of being placed on their side. n = 6 per group.

2.7. Motor performance

Motor performance was assessed using an accelerating rotarod device (model 7650; Ugo Basile, Gemonio VA, Italy). Mice were trained for three consecutive days prior to the start of the recording. The mice ran on the rotarod for over 2 min and measurements were performed six times per week from when the mice were eight weeks old until the mice were unable to remain on the rotarod for more than 10 s. The best values of three trials were scored. A 15-min rest was allowed between trials. n = 7 per group.

2.8. Nissl staining and immunohistochemistry

Isoflurane-anesthetized mice were perfused with pre-chilled PBS, and the lumbar spinal cords were embedded in Tissue-Tek O.C.T. compound (Sakura FineTek, Tokyo, JPN, cat#4583). For the Nissl staining, fresh frozen 20-μm sections were stained in 0.1 %

cresyl violet (Muto Pure Chemicals Co. Ltd., Tokyo, JPN, cat#4102-2) with 0.1 % acetic acid at room temperature for 5 min and rinsed with 95 % ethanol with a few drops of 10 % acetic acid for 10 min. After that, the sections were penetrated and enclosed by Entellan new (Merck Millipore, Burlington, MA, USA, cat#107961). Images of the sections were captured using a brightfield microscope BZ-9000 (Keyence, Osaka, JPN), and the number of motor neurons was manually quantified as the average of six sections that were randomly selected.

For immunohistochemistry, fresh frozen 20-μm sections were fixed using 4 % paraformaldehyde (Nacalai Tesque, cat#26126-25) in PBS for 20 min, washed in PBS twice every 2 min, and finally washed in PBS with 0.3 % Triton X-100 (PBST) for 2 min. Sections were blocked using BlockingOne (Nacalai Tesque, cat#03953-95) at room temperature for 30 min or 5 % normal goat serum with PBST at room temperature for 1 h. The sections were next incubated with primary antibodies in 5 % BlockingOne with PBST at 4 °C overnight (~16 h). After washing the sections with PBST three times for 5 min, they were exposed to goat or donkey secondary antibodies conjugated to Alexa Fluor 488 (Thermo Fisher Scientific, Waltham, MA, USA, cat#A32731 or cat#A21202) or 647 (Thermo Fisher Scientific, cat#A31573) at a 1:1,000 dilution in 5 % BlockingOne with PBST for 1 h at room temperature. The sections were then washed in PBST twice for 5 min and subsequently in PBS for 5 min at room temperature. The sections were mounted on coverslips with ProLong Diamond Antifade Mountant with 4',6-diamidino-2-phenylindole (DAPI; Thermo Fisher Scientific, cat#P36952), and images were captured using a fluorescence microscope BZ-9000 (Keyence), fluorescence microscope BZ-X710 (Keyence), or fluorescence confocal microscope FV-1000 (OLYMPUS, Tokyo, JPN). The expression levels of glial activation markers and 4-hydroxy-2-nonenal (4-HNE) were quantified as fluorescence intensities from an average of three randomly selected sections using ImageJ/Fiji (version 2.0.0, RRID:SCR_002285) software. The primary antibodies used for immunohistochemistry were rabbit anti-4-HNE (1:200; Abcam, cat#ab46545, RRID:AB_722490), rab-

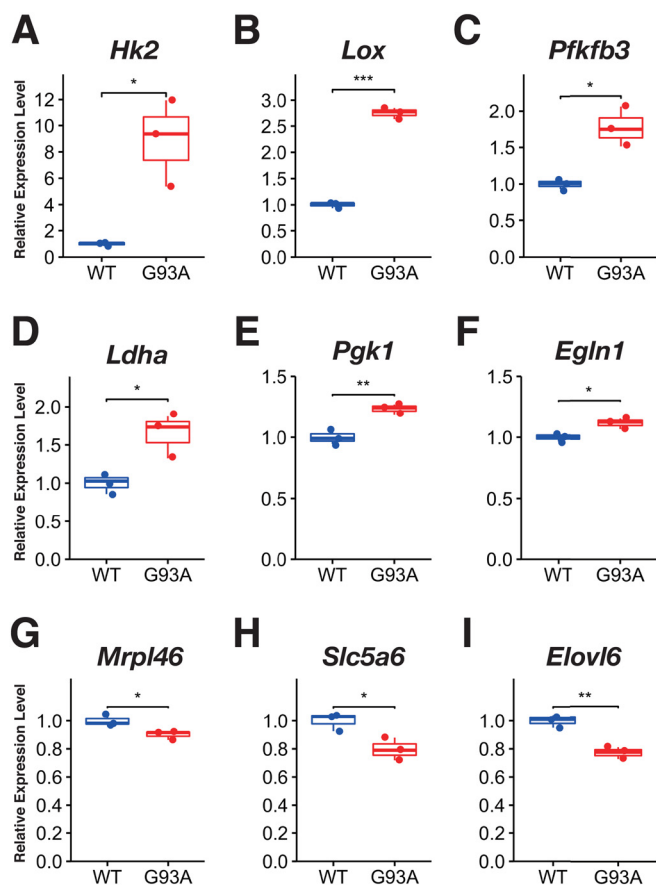


Fig. 2. Hypoxia-related genes are altered in familial ALS model mice. RT-qPCR analysis was performed to analyze the expression of hypoxia-related genes in the spinal cord of wild-type (WT) and littermate $SOD1^{G93A}$ mice. (A) *Hk2*, (B) *Lox*, (C) *Pfkfb3*, (D) *Ldha*, (E) *Pkg1*, (F) *Egl1*, (G) *Mrpl46*, (H) *Slc5a6*, (I) *Elovl6*. The expression levels were normalized to *Gapdh* expression. $n = 3$ mice per group. Data are presented as box plot and dot plots normalized to the wild-type group. *: $p < 0.05$. **: $p < 0.01$. ***: $p < 0.001$. Student's *t*-test. Abbreviation: G93A, $SOD1^{G93A}$.

bit anti-Iba1 (1:500; Wako, cat#019-19741), mouse anti-GFAP (1:500; Sigma-Aldrich, cat#G3893, RRID:AB_47710), and mouse anti-SLC5A6 (1:1,000; Santa Cruz Biotechnology, Dallas, TX, USA, cat#sc-390080). $n = 4$ per group.

2.9. Statistical analysis

All data are presented as the mean \pm standard error of the mean (SEM) or as box plots with dot plots. Statistical analyses were performed using R (Version 3.5.1) and MATLAB (Version R2018a, RRID:SCR.001622) software. We used the one-way analysis of variance (ANOVA) followed by Tukey's multiple comparison test for multiple groups comparisons and Student's *t*-test for comparisons between two groups. Analyses of disease onset and survival period were performed using the log-rank test, and no sample size calculation was performed in this study. Differences with $p < 0.05$ were considered to be statistically significant.

3. Results

3.1. 6-Deoxyjacareubin protects against non-apoptotic cell death by inhibiting ROS production

We confirmed that 6-deoxyjacareubin inhibited cytotoxicity induced by sealed chamber hypoxia (1 % O_2) and chemically induced hypoxia ($CoCl_2$) in HEK293T cells and other types of cell

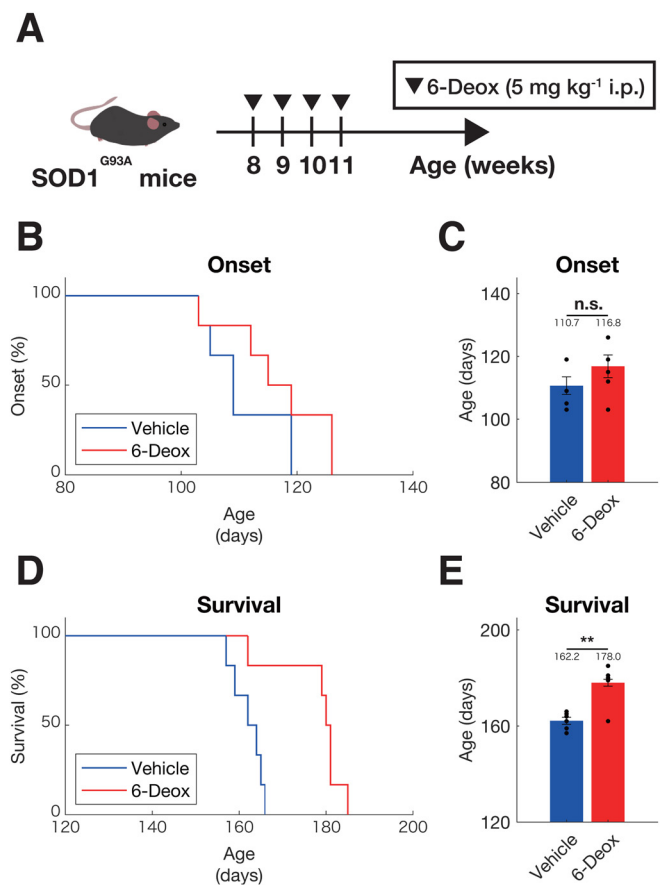


Fig. 3. 6-Deoxyjacareubin prolongs the survival of familial ALS model mice. (A) 6-Deoxyjacareubin injection schedule. $SOD1^{G93A}$ mice (eight weeks old) were injected i.p. with either vehicle or 6-deoxyjacareubin (5 mg kg^{-1}) every week for 1 month. (B) Kaplan-Meier curves for the disease onset time in $SOD1^{G93A}$ mice treated with either vehicle (blue; $n = 6$ per group) or 6-deoxyjacareubin (red; $n = 6$ per group). (C) Plotted mean onset time. (D) Kaplan-Meier curves for the survival time of $SOD1^{G93A}$ mice treated with either vehicle (blue; $n = 6$ per group) or 6-deoxyjacareubin (red; $n = 6$ per group). (E) Plotted mean survival time. Data are presented as the mean \pm SEM. **: $p < 0.01$. n.s., not significant. Log-rank test. Abbreviation: 6-Deox, 6-deoxyjacareubin.

lines such as HT1080 (human sarcoma cell line), Neuro2a (mouse neuroblastoma cell line), and MO3.13 (human oligodendrocytic cell line) (Fig. 1A–C, Supplementary Fig. S1A–D). Subsequently, we determined whether 6-deoxyjacareubin could prevent intracellular ROS generation, because hypoxia increases ROS production (Tafari et al., 2016). As shown in Supplementary Fig. S2A, B, 6-deoxyjacareubin inhibited ROS production after exposure to $CoCl_2$. To further analyze the specificity of 6-deoxyjacareubin in greater detail, we evaluated the protective effects of 6-deoxyjacareubin against various agents that induce cell death. As shown in Fig. 1D–F, 6-deoxyjacareubin did not protect cells against the effects of staurosporine (apoptosis), H_2O_2 (mainly necrosis), or erastin (ferroptosis). Since 6-deoxyjacareubin is known to be a PAFR inhibitor (Jantan et al., 2002; Oku et al., 2005), we also checked whether the well-known PAFR inhibitors, WEB-2086 and ginkgolide B, suppress hypoxia-induced cell death. However, neither WEB-2086 nor ginkgolide B influenced cell death initiated by chemically induced hypoxia ($CoCl_2$) (Supplementary Fig. S3A, B). Finally, we checked the expression levels of HIF-1 α and found that 6-deoxyjacareubin did not change HIF-1 α expression (Supplementary Fig. S4A, B). These results suggest that 6-deoxyjacareubin acts as a protective agent against non-apoptotic cell death by inhibiting ROS generation under hypoxic conditions.

3.2. 6-Deoxyjacareubin prolongs the survival time of SOD1^{G93A} mice and improves their locomotor dysfunction

To confirm that hypoxia occurs in the ALS model, we used RT-qPCR to first examine the expression levels of hypoxia-responsive genes in the spinal cord of SOD1^{G93A} mice. Using published reports on RNA-seq and microarrays, we evaluated the expression levels of several genes known to be altered after sealed chamber hypoxia and chemically induced hypoxia (CoCl₂) (Calvo-Anguiano et al., 2018; Cavadas et al., 2016; Zhigalova et al., 2015). We observed that the expression levels of several hypoxia-related genes such as *Lox*, *Ldha*, and *Hk2* were altered in end-stage SOD1^{G93A} mice (Fig. 2A-I).

To evaluate the therapeutic effects of 6-deoxyjacareubin in SOD1^{G93A} mice, 6-deoxyjacareubin (5 mg kg⁻¹) or vehicle (10 % DMSO and 10 % Cremophor EL in saline) was injected i.p. into SOD1^{G93A} mice (Fig. 3A). Because spinal blood flow is impaired at presymptomatic stages (Miyazaki et al., 2012, 2011), the drugs were administered weekly from the age of eight weeks. We also confirmed that no obvious phenotypic or toxic changes, such as a loss of body weight, were observed in the WT mice by injecting vehicle or 6-deoxyjacareubin (Supplementary Fig. S5). Although 6-deoxyjacareubin administration showed only a tendency to delay the onset time in SOD1^{G93A} mice (vehicle group: 110.7 ± 8.3 days; 6-deoxyjacareubin group: 116.8 ± 9.2 days; Fig. 3B, C), the compound significantly increased the survival time in SOD1^{G93A} mice by ~16 days (vehicle group: 162.2 ± 3.8 days; 6-deoxyjacareubin group: 178.0 ± 7.0 days; Fig. 3D, E).

Because SOD1^{G93A} mice show progressive locomotor dysfunction due to loss of motor neurons, we also performed the rotarod test. In the vehicle group, locomotor function progressively declined, but administration of 6-deoxyjacareubin attenuated this decline (Fig. 4, Supplementary Video). We also confirmed that 6-deoxyjacareubin suppressed the abnormal limb-clasping reflex by tail suspension (Supplementary Fig. S6). These results suggest that 6-deoxyjacareubin has neuroprotective effects.

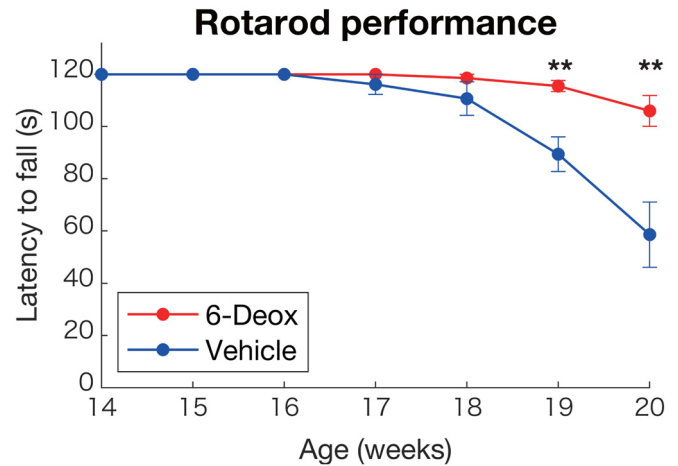


Fig. 4. 6-Deoxyjacareubin prevents deterioration of locomotor function in familial ALS model mice. Rotarod performance of SOD1^{G93A} mice treated with either vehicle (blue; n = 7 per group) or 6-deoxyjacareubin (red; n = 7 per group). Data are presented as the mean ± SEM. **: p < 0.01. Student's *t*-test. Abbreviation: 6-Deox, 6-deoxyjacareubin.

3.3. 6-Deoxyjacareubin attenuates motor neuron loss and suppresses glial activation in end-stage SOD1^{G93A} mice

To assess the pathology of SOD1^{G93A} mice, we next performed Nissl staining. Severe motor neuron loss (70.8 % reduction) was observed at the end stage in vehicle-treated SOD1^{G93A} mice. By contrast, significant recovery was observed in 6-deoxyjacareubin-treated SOD1^{G93A} mice (32.0 % improvement; Fig. 5A, B). It is known that oxidative stress-related products such as 4-HNE, a lipid peroxidation product often used as an oxidative stress marker, accumulate in motor neurons of ALS model mice (Kim et al., 2009). Therefore, we performed immunostaining against 4-HNE to assess the effects of 6-deoxyjacareubin on oxidative stress in motor neurons. As shown in Supplementary Fig. S7A, B, less 4-HNE accumulation was seen in 6-deoxyjacareubin-treated SOD1^{G93A} mice. These results suggest that 6-deoxyjacareubin protects motor neurons by dampening oxidative stress.

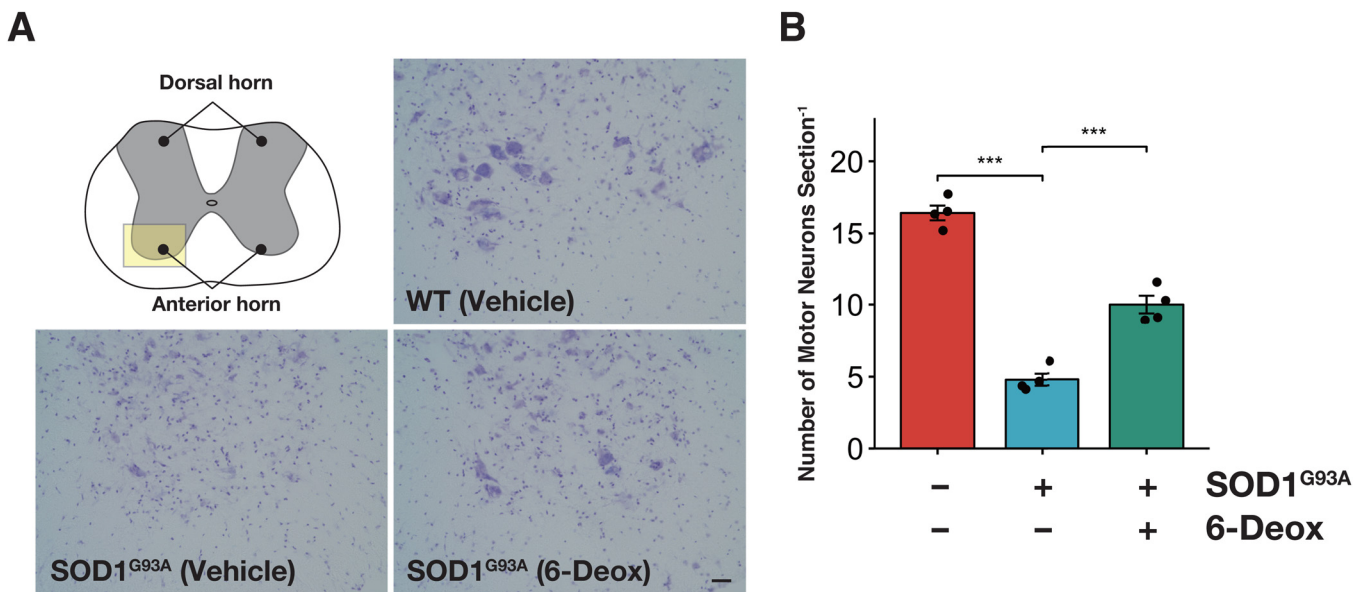


Fig. 5. 6-Deoxyjacareubin attenuates motor neuron loss in familial ALS model mice. (A, B) End-stage SOD1^{G93A} mice and their wild-type (WT) littermates treated with either vehicle or 6-deoxyjacareubin. (A) Representative images of Nissl-stained ventral horns of the lumbar spinal cord. Scale bar: 40 μm. (B) Quantification of the data presented in (A). n = 4 per group. Data are presented as the mean ± SEM. ***: p < 0.001. n.s.: not significant. One-way ANOVA followed by Tukey's post hoc test. Abbreviation: 6-Deox, 6-deoxyjacareubin.

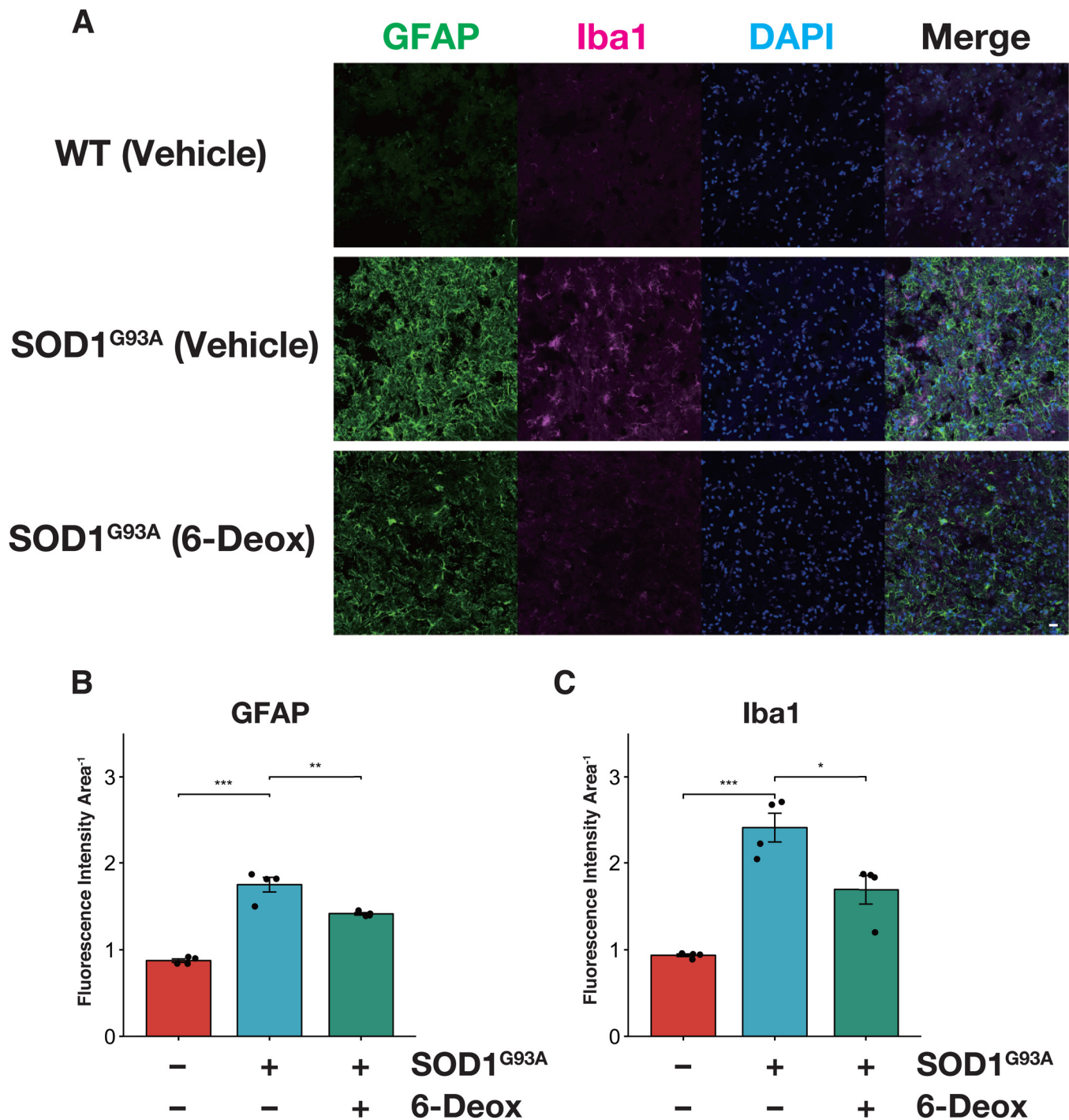


Fig. 6. 6-Deoxyjacareubin prevents glial activation in familial ALS model mice. (A–C) Wild-type (WT) and end-stage SOD1^{G93A} mice treated with either vehicle or 6-deoxyjacareubin. (A) Representative images of immunofluorescence staining for GFAP (astrocyte marker) and Iba1 (microglial marker) in the ventral horns of the lumbar spinal cord. Scale bar: 40 μ m. (B, C) Quantification of the data in (A). n = 4 per group. Data are presented as the mean \pm SEM normalized to the WT group. *: p < 0.05. **: p < 0.01. ***: p < 0.001. One-way ANOVA followed by Tukey's post hoc test. Abbreviations: 6-Deox, 6-deoxyjacareubin.

To examine the effects of 6-deoxyjacareubin in glial cells, we performed immunostaining using antibodies against ionized calcium-binding adapter molecule 1 (Iba1; microglial marker) and glial fibrillary acidic protein (GFAP; astrocyte marker). We observed generalized glial activation in the form of increased microglial and astrocyte-specific staining in the spinal cord of vehicle-treated SOD1^{G93A} mice (Fig. 6A–C). By contrast, activation of microglia and astrocytes was attenuated in the 6-deoxyjacareubin-treated group (Fig. 6A–C). These results indicate that 6-deoxyjacareubin

suppresses glial activation in addition to its protective effect on motor neuron loss.

3.4. Downregulation of *Slc5a6* expression improved after treatment with 6-deoxyjacareubin in end-stage SOD1^{G93A} mice

Finally, we assessed the expression levels of hypoxia-responsive genes (Fig. 2A–I) in the spinal cord of SOD1^{G93A} mice treated with vehicle or 6-deoxyjacareubin, to examine the effects of hypoxia-

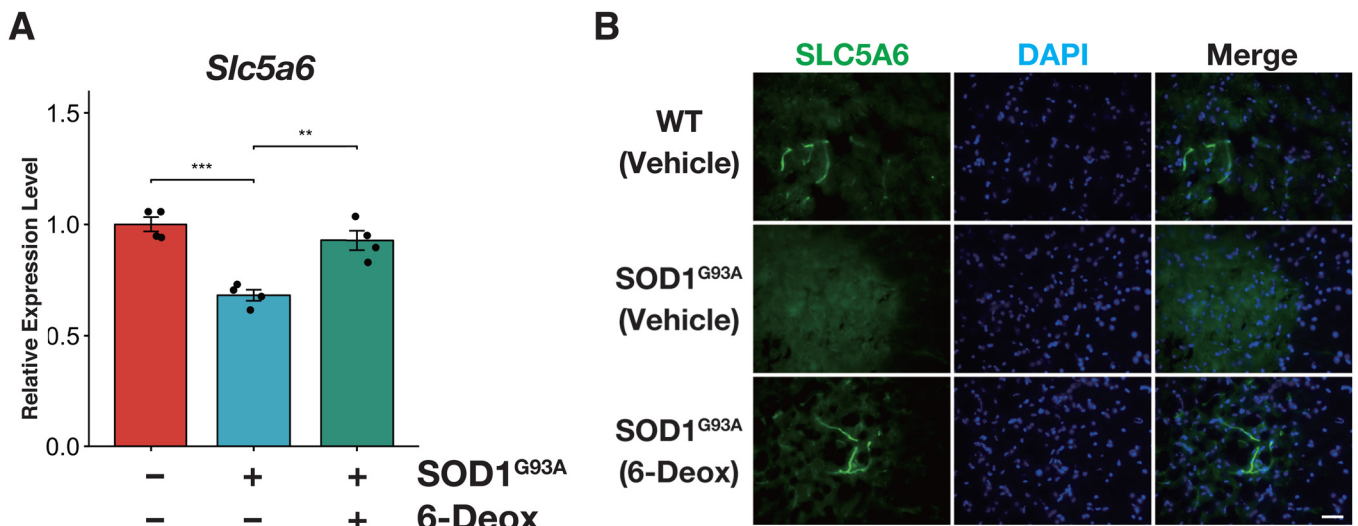


Fig. 7. Downregulation of *Slc5a6* expression improved after treatment with 6-deoxyjacareubin in familial ALS model mice. (A) RT-qPCR analysis of the expression of *Slc5a6* in the spinal cord of wild-type (WT) and end-stage *SOD1^{G93A}* mice treated with either vehicle or 6-deoxyjacareubin. The expression levels were normalized to those of *Gapdh*. $n = 4$ mice per group. Data are presented as the mean \pm SEM normalized to the WT group. **: $p < 0.01$. ***: $p < 0.001$. One-way ANOVA followed by Tukey's post hoc test. (B) Representative images of immunofluorescence staining for SLC5A6 in the ventral horns of the lumbar spinal cord. Scale bar: 40 μ m. Abbreviation: 6-Deox, 6-deoxyjacareubin.

related genes in ALS model mice. We found that the downregulation of the solute carrier family 5 member 6 (*Slc5a6*) gene improved in 6-deoxyjacareubin-treated *SOD1^{G93A}* mice using RT-qPCR (Fig. 7A). Furthermore, we also conducted immunostaining of SLC5A6 and 6-deoxyjacareubin also recovered in 6-deoxyjacareubin-treated *SOD1^{G93A}* mice (Fig. 7B). These results are suggestive of the neuroprotective effects of 6-deoxyjacareubin.

4. Discussion

In this study, we revealed that 6-deoxyjacareubin ameliorated disease progression in *SOD1^{G93A}* mice. Although hypoxia has been implicated in neurodegenerative diseases, the effect of treating hypoxia in these diseases remains unknown. Using the small-molecule drug 6-deoxyjacareubin, this study demonstrates that suppression of hypoxia-induced damage is an effective therapeutic strategy in *SOD1^{G93A}* mice. However, the functional mechanisms of the effects of 6-deoxyjacareubin on hypoxia remain unclear. 6-Deoxyjacareubin is known to be a PAFR inhibitor (Jantan et al., 2002; Oku et al., 2005). However, the well-characterized PAFR inhibitors, WEB-2086 and ginkgolide B, did not suppress hypoxia-induced cell death (Supplementary Fig. S3A, B). Therefore, 6-deoxyjacareubin exerts its protective effects on hypoxia-induced cell death via PAFR-independent pathways. We also found that 6-deoxyjacareubin did not suppress apoptosis (Fig. 1D). In support of this, 6-deoxyjacareubin did not completely inhibit hypoxia-induced cell death (Fig. 1B, C), because both apoptotic and non-apoptotic cell death occur under hypoxic conditions (Shimizu et al., 1996). These observations suggest that the neuroprotective effects of 6-deoxyjacareubin is due to effects on non-apoptotic cell death. Recent studies have revealed that non-apoptotic cell death plays an important role in the pathogenesis of neurodegenerative diseases including ALS (Guégan and Przedborski, 2003; Ito et al., 2016; Kim et al., 2019; Morrice et al., 2017). Thus, suppression of non-apoptotic cell death by 6-deoxyjacareubin may be a useful strategy to develop new therapies. However, this study was unable to determine exactly which non-apoptotic cell death pathway is suppressed by 6-deoxyjacareubin. Accordingly, future studies will need to identify the 6-deoxyjacareubin targets along with their functions.

Since spinal blood flow is impaired at early presymptomatic stages in *SOD1^{G93A}* mice (Miyazaki et al., 2012), we administered 6-deoxyjacareubin to eight weeks old mice for 1 month. At this stage, oxidative stress is also increased in *SOD1^{G93A}* mice (Casoni et al., 2005; Chang et al., 2008). Because 6-deoxyjacareubin strongly inhibited ROS production induced by chemical hypoxia (Supplementary Fig. S2A, B), its neuroprotective effects may be due to suppression of ROS production. Moreover, oxidative stress increases in neurons and glial cells during the progression of neurodegenerative diseases (Casoni et al., 2005; Kim et al., 2009; Thonhoff et al., 2012). Activated glial cells, such as astrocytes and microglia, play important roles in neurodegenerative diseases through a non-cell-autonomous mechanism (Ilieva et al., 2009; Lasiene and Yamanaka, 2011). Thus, 6-deoxyjacareubin may have a neuroprotective effect by preventing cell death of motor neurons and by suppressing glial activation via inhibition of ROS production. Furthermore, we found that downregulation of *Slc5a6* improved in *SOD1^{G93A}* mice after treatment with 6-deoxyjacareubin (Fig. 2H and 7A, B). Single-cell RNA-seq data from the mouse nervous system have revealed that *Slc5a6* is highly expressed in vascular leptomeningeal cells involved in the neurovascular unit (Zeisel et al., 2018). SLC5A6, a sodium-dependent multivitamin transporter, is involved in the transportation of water-soluble vitamins such as biotin and pantothenic acid across the blood-brain barrier (BBB) (Uchida et al., 2015). Since neurovascular units and the BBB are disrupted in ALS model mice (Garbuzova-Davis et al., 2007; Miyazaki et al., 2011), 6-deoxyjacareubin may also play a protective role in the neurovascular unit and/or the BBB.

HIF-1 α , which is normally exposed to rapid proteolysis, translocates under hypoxic conditions into the nucleus and induces the expression of genes downstream of HIF-1 α such as *Hmox1*, *Vegfa*, and *Hk2*. However, nuclear localization of HIF-1 α is impaired in ALS model mice and in patients with ALS, despite increased expression of HIF-1 α in motor neurons (Nagara et al., 2013; Sato et al., 2012). Therefore, a HIF-1 α -independent pathway may be an adequate target for ALS therapies. Since 6-deoxyjacareubin did not increase HIF-1 α expression (Supplementary Fig. S4A, B), it may have effects other than acting as a HIF-1 α activator.

Thus, these findings suggest that the inhibition of hypoxia-induced cell death may be a potential strategy for ALS treatment. Hypoxia has been implicated in various other neurodegenera-

tive diseases such as Alzheimer's disease and Parkinson's disease (Asllani et al., 2008; Foti et al., 2010; Gutiérrez-Jiménez et al., 2018; Iturria-Medina et al., 2016; Love and Miners, 2016; Nielsen et al., 2017; Nortley et al., 2019; Zeisel et al., 2018), suggesting that 6-deoxyjacareubin may benefit these diseases as well. In the future, further studies using models of other neurodegenerative diseases will be required.

5. Conclusions

We demonstrated that treatment with 6-deoxyjacareubin prevented hypoxia-induced cell death and significantly prolonged the survival time of a mouse model of familial ALS by attenuating motor neuron loss and glial activation. Consequently, the present study provides evidence that hypoxia treatment, such as using 6-deoxyjacareubin, might be a potential therapeutic strategy for hypoxia-related neurodegenerative diseases such as ALS.

Author contributions

T.H. and S.M. designed the experiments. T.H. performed the experiments and analyzed the data. T.H. prepared and assembled the figures. T.H. wrote the manuscript. S.M. and R.T. managed the project. S.M. and R.T. provided critical reading and scientific discussions. All authors reviewed and approved the final version of this manuscript.

Role of the funding source

This work was supported by a Grant-in-Aid from the Japan Society for the Promotion of Science (JSPS) Fellows (Grant Number 17J05111 to T.H.) and funding from the Project of Translational and Clinical Research Core Centers from the Japan Agency for Medical Research and Development (AMED; Grant Number 18lm0203006j0002 to S.M.). This work was mainly performed at the Drug Screening Incubation Laboratory, Graduate School of Medicine, Kyoto University. Experiments using the BZ-9000 (Keyence), BZ-X710 (Keyence), ARVO X5 (PerkinElmer), FACS LSRFortessa (BD Biosciences), FlowJo Software (FlowJo), and ChemiDocMP (Bio-Rad) were performed at the Medical Research Support Center, Graduate School of Medicine, Kyoto University, which was supported by the Platform for Drug Discovery, Informatics, and Structural Life Science from the Ministry of Education, Culture, Sports, Science and Technology, Japan.

Declaration of Competing Interest

The authors declare no competing financial interests.

Acknowledgements

We thank Keiko Imamura and Haruhisa Inoue (Center for iPS Cell Research and Application (CiRA), Kyoto University, Kyoto 606-8507, Japan) for help with experiments and providing critical discussion. We also thank our colleagues at the Department of Neurology, Graduate School of Medicine, Kyoto University.

Appendix A. Supplementary data

Supplementary material related to this article can be found, in the online version, at doi:<https://doi.org/10.1016/j.neures.2020.02.011>.

References

- Asllani, I., Habeck, C., Scarmeas, N., Borogovac, A., Brown, T.R., Stern, Y., 2008. Multivariate and univariate analysis of continuous arterial spin labeling perfusion MRI in Alzheimer's disease. *J. Cereb. Blood Flow Metab.* 28, 725–736. <http://dx.doi.org/10.1038/sj.cbfm.9600570>.
- Barber, S.C., Mead, R.J., Shaw, P.J., 2006. Oxidative stress in ALS: a mechanism of neurodegeneration and a therapeutic target. *Biochim. Biophys. Acta - Mol. Basis Dis.* 1762, 1051–1067. <http://dx.doi.org/10.1016/j.bbadis.2006.03.008>.
- Brown, R.H., Al-Chalabi, A., 2017. Amyotrophic lateral sclerosis. *N. Engl. J. Med.* 377, 162–172. <http://dx.doi.org/10.1056/NEJMr1603471>.
- Calvo-Anguiano, G., Lugo-Trampe, J.J., Camacho, A., Said-Fernández, S., Mercado-Hernández, R., Zomosa-Signoret, V., Rojas-Martínez, A., Ortiz-López, R., 2018. Comparison of specific expression profile in two in vitro hypoxia models. *Exp. Ther. Med.* 15, 4777–4784. <http://dx.doi.org/10.3892/etm.2018.6048>.
- Casoni, F., Basso, M., Massignan, T., Gianazza, E., Cheroni, C., Salmona, M., Bendotti, C., Bonetto, V., 2005. Protein nitration in a mouse model of familial amyotrophic lateral sclerosis: possible multifunctional role in the pathogenesis. *J. Biol. Chem.* 280, 16295–16304. <http://dx.doi.org/10.1074/jbc.M413111200>.
- Cavadas, M.A.S., Mesnieres, M., Crifo, B., Manresa, M.C., Selfridge, A.C., Keogh, C.E., Fabian, Z., Scholz, C.C., Nolan, K.A., Rocha, L.M.A., Tambuwala, M.M., Brown, S., Wdowicz, A., Corbett, D., Murphy, K.J., Godson, C., Cummins, E.P., Taylor, C.T., Cheong, A., 2016. REST is a hypoxia-responsive transcriptional repressor. *Sci. Rep.* 6, 31355. <http://dx.doi.org/10.1038/srep31355>.
- Chang, Y., Kong, Q., Shan, X., Tian, G., Ilieva, H., Cleveland, D.W., Rothstein, J.D., Borchelt, D.R., Wong, P.C., Lin, C.G., 2008. Messenger RNA oxidation occurs early in disease pathogenesis and promotes motor neuron degeneration in ALS. *PLoS One* 3, e2849. <http://dx.doi.org/10.1371/journal.pone.0002849>.
- Doriguetto, A.C., Santos, M.H., Ellena, J.A., Nagem, T.J., 2001. 6-Deoxyjacareubin. *Acta Crystallogr. C* 57, 1095–1097. <http://dx.doi.org/10.1107/s0108270101009246>.
- Endo, F., Komine, O., Fujimori-Tonou, N., Katsuno, M., Jin, S., Watanabe, S., Sobue, G., Dezaawa, M., Wyss-Coray, T., Yamanaka, K., 2015. Astrocyte-derived TGF- β 1 accelerates disease progression in ALS mice by interfering with the neuroprotective functions of microglia and T cells. *Cell Rep.* 11, 592–604. <http://dx.doi.org/10.1016/j.celrep.2015.03.053>.
- Foti, R., Zucchelli, S., Biagioli, M., Roncaglia, P., Vilotti, S., Calligaris, R., Krmac, H., Girardini, J.E., Del Sal, G., Gustincich, S., 2010. Parkinson disease-associated DJ-1 is required for the expression of the glial cell line-derived neurotrophic factor receptor RET in human neuroblastoma cells. *J. Biol. Chem.* 285, 18565–18574. <http://dx.doi.org/10.1074/jbc.M109.088294>.
- Garbuzova-Davis, S., Haller, E., Saporta, S., Kolomey, I., Nicosia, S.V., Sanberg, P.R., 2007. Ultrastructure of blood-brain barrier and blood-spinal cord barrier in SOD1 mice modeling ALS. *Brain Res.* 1157, 126–137. <http://dx.doi.org/10.1016/j.brainres.2007.04.044>.
- Girouard, H., Iadecola, C., 2006. Neurovascular coupling in the normal brain and in hypertension, stroke, and Alzheimer disease. *J. Appl. Physiol.* 100, 328–335. <http://dx.doi.org/10.1152/jappphysiol.00966.2005>.
- Guégan, C., Przedborski, S., 2003. Programmed cell death in amyotrophic lateral sclerosis. *J. Clin. Invest.* 111, 153–161. <http://dx.doi.org/10.1172/JCI200317610>.
- Gutiérrez-Jiménez, E., Angleys, H., Rasmussen, P.M., West, M.J., Catalini, L., Iversen, N.K., Jensen, M.S., Frische, S., Østergaard, L., 2018. Disturbances in the control of capillary flow in an aged APPswe/PS1 Δ E9 model of Alzheimer's disease. *Neurobiol. Aging* 62, 82–94. <http://dx.doi.org/10.1016/j.neurobiolaging.2017.10.006>.
- Ilieva, H., Polymenidou, M., Cleveland, D.W., 2009. Non-cell autonomous toxicity in neurodegenerative disorders: ALS and beyond. *J. Cell Biol.* 187, 761–772. <http://dx.doi.org/10.1083/jcb.200908164>.
- Ito, Y., Ofengeim, D., Najafav, A., Das, S., Saberi, S., Li, Y., Hitomi, J., Zhu, H., Chen, H., Mayo, L., Geng, J., Amin, P., DeWitt, J.P., Mookhtiar, A.K., Florez, M., Ouchida, A.T., Fan, J., Pasparakis, M., Kelliher, M.A., Ravits, J., Yuan, J., 2016. RIPK1 mediates axonal degeneration by promoting inflammation and necroptosis in ALS. *Science* 353, 603–608. <http://dx.doi.org/10.1126/science.aaf6803>.
- Iturria-Medina, Y., Sotero, R.C., Toussaint, P.J., Mateos-Pérez, J.M., Evans, A.C., Weiner, M.W., Aisen, P., Petersen, R., Jack, C.R., Jagust, W., Trojanowski, J.Q., Toga, A.W., Beckett, L., Green, R.C., Saykin, A.J., Morris, J., Shaw, L.M., Khachaturian, Z., Sorensen, G., Kuller, L., Raichle, M., Paul, S., Davies, P., Fillit, H., Hefti, F., Holtzman, D., Mesulam, M., Marcel, Potter, W., Snyder, P., Schwartz, A., Montine, T., Thomas, R.G., Donohue, M., Walter, S., Gessert, D., Sather, T., Jimenez, G., Harvey, D., Bernstein, M., Fox, N., Thompson, P., Schuff, N., Borowski, B., Gunter, J., Senjem, M., Vemuri, P., Jones, D., Kantarci, K., Ward, C., Koepp, R.A., Foster, N., Reiman, E.M., Chen, K., Mathis, C., Landau, S., Cairns, N.J., Householder, E., Taylor-Reinwald, L., Lee, V., Korecka, M., Figurski, M., Crawford, K., Neu, S., Foroud, T.M., Potkin, S., Shen, L., Faber, K., Kim, S., Nho, K., Thal, L., Buckholtz, N., Albert, Marilyn, Frank, R., Hsiao, J., Kaye, J., Quinn, J., Lind, B., Carter, R., Dolen, S., Schneider, L.S., Pawluczyk, S., Beccera, M., Teodoro, L., Spann, B.M., Brewer, J., Vanderswag, H., Fleisher, A., Heidebrink, J.L., Lord, J.L., Mason, S.S., Albers, C.S., Knopman, D., Johnson, Kris, Doody, R.S., Villanueva-Meyer, J., Chowdhury, M., Rountree, S., Dang, M., Stern, Y., Honig, L.S., Bell, K.L., Ances, B., Carroll, M., Leon, S., Mintun, M.A., Schneider, S., Oliver, A., Marson, D., Griffith, R., Clark, D., Geldmacher, D., Brockington, J., Roberson, E., Grossman, H., Mitsis, E., De Toledo-Morrell, L., Shah, R.C., Duara, R., Varon, D., Greig, M.T., Roberts, P., Albert, Marilyn, Onyike, C., D'Agostino, D., Kiehl, S., Galvin, J.E., Cerbone, B., Michel, C.A., Rusinek, H., De Leon, M.J., Glodzik, L., De Santi, S., Doraiswamy, P.M., Petrella, J.R., Wong, T.Z., Arnold, S.E., Karlawish, J.H., Wolk, D., Smith, C.D., Jicha, G., Hardy, P., Sinha, P., Oates, E., Conrad, G., Lopez, O.L., Oakley, M., Simpson, D.M., Porsteinsson, A.P., Goldstein, B.S., Martin, K., Makino, K.M., Ismail, M.S., Brand, C., Mulnard, R.A., Thai, G., Mc-Adams-Ortiz, C., Womack, K., Mathews, D., Quiceno, M., Diaz-

- Arrastia, R., King, R., Weiner, M., Martin-Cook, K., DeVous, M., Levey, A.I., Lah, J.J., Cellar, J.S., Burns, J.M., Anderson, H.S., Swerdlow, R.H., Apostolova, L., Tingus, K., Woo, E., Silverman, D.H.S., Lu, P.H., Bartzokis, G., Graff-Radford, N.R., Parfitt, F., Kendall, T., Johnson, H., Farlow, M.R., Hake, A., Matthews, B.R., Herring, S., Hunt, C., Van Dyck, C.H., Carson, R.E., MacAvoy, M.G., Chertkow, H., Bergman, H., Hosein, C., Black, S., Stefanovic, B., Caldwell, C., Hsiung, G.Y.R., Feldman, H., Mudge, B., Assaly, M., Kertesz, A., Rogers, J., Bernick, C., Muncie, D., Kerwin, D., Mesulam, Marek Marsel, Lipowski, K., Wu, C.K., Johnson, N., Sadowsky, C., Martinez, W., Villena, T., Turner, R.S., Johnson, Kathleen, Reynolds, B., Sperling, R.A., Johnson, K.A., Marshall, G., Frey, M., Lane, B., Rosen, A., Tinklenberg, J., Sabbagh, M.N., Belden, C.M., Jacobson, S.A., Sirrel, S.A., Kowall, N., Killiany, R., Budson, A.E., Norbath, A., Johnson, P.L., Allard, J., Lerner, A., Ogrocki, P., Hudson, L., Fletcher, E., Carmichael, O., Olichney, J., DeCarli, C., Kittur, S., Borrie, M., Lee, T.Y., Bartha, R., Johnson, S., Asthana, S., Carlsson, C.M., Potkin, S.G., Preda, A., Nguyen, D., Tariot, P., Reeder, S., Bates, V., Capote, H., Rainka, M., Scharre, D.W., Katakai, M., Adeli, A., Zimmerman, E.A., Celmins, D., Brown, A.D., Pearson, G.D., Blank, K., Anderson, K., Santulli, R.B., Kitzmiller, T.J., Schwartz, E.S., Sink, K.M., Williamson, J.D., Garg, P., Watkins, F., Ott, B.R., Querfurth, H., Tremont, G., Salloway, S., Malloy, P., Correia, S., Rosen, H.J., Miller, B.L., Mintzer, J., Spicer, K., Bachman, D., Finger, E., Pasternak, S., Rachinsky, I., Drost, D., Pomara, N., Hernando, R., Sarrael, A., Schultz, S.K., Ponto, L.L.B., Shim, H., Smith, K.E., Relkin, N., Chaing, G., Raudin, L., Smith, A., Fargher, K., Raj, B.A., Neylan, T., Grafman, J., Davis, M., Morrison, R., Hayes, J., Finley, S., Friedl, K., Fleischman, D., Arfanakis, K., James, O., Massoglia, D., Fruehling, J.J., Harding, S., Peskind, E.R., Petrie, E.C., Li, G., Yesavage, J.A., Taylor, J.L., Furst, A.J., 2016. Early role of vascular dysregulation on late-onset Alzheimer's disease based on multifactorial data-driven analysis. *Nat. Commun.* 7, <http://dx.doi.org/10.1038/ncomms11934>.
- Iyer, N.V., Kotch, L.E., Agani, F., Leung, S.W., Laughner, E., Wenger, R.H., Gassmann, M., Gearhart, J.D., Lawler, A.M., Yu, A.Y., Semenza, G.L., 1998. Cellular and developmental control of O₂ homeostasis by hypoxia-inducible factor 1 alpha. *Genes Dev.* 12, 149–162, <http://dx.doi.org/10.1101/gad.12.2.149>.
- Jantan, I., Pizar, M.M., Idris, M.S., Taher, M., Ali, R.M., 2002. In vitro inhibitory effect of rubraxanthone isolated from *Garcinia parvifolia* on platelet-activating factor receptor binding. *Planta Med.* 68, 1133–1134, <http://dx.doi.org/10.1055/s-2002-36343>.
- Kim, J., Kim, T.Y., Hwang, J.J., Lee, J.Y., Shin, J.H., Gwag, B.J., Koh, J.Y., 2009. Accumulation of labile zinc in neurons and astrocytes in the spinal cords of G93A SOD-1 transgenic mice. *Neurobiol. Dis.* 34, 221–229, <http://dx.doi.org/10.1016/j.nbd.2009.01.004>.
- Kim, S.-M., Kim, H., Lee, J.-S., Park, K.S., Jeon, G.S., Shon, J., Ahn, S.-W., Kim, S.H., Lee, K.M., Sung, J.-J., Lee, K.-W., 2013. Intermittent hypoxia can aggravate motor neuronal loss and cognitive dysfunction in ALS mice. *PLoS One* 8, e81808, <http://dx.doi.org/10.1371/journal.pone.0081808>.
- Kim, E.H., Wong, S.-W., Martinez, J., 2019. Programmed necrosis and disease: we interrupt your regular programming to bring you necroinflammation. *Cell Death Differ.* 26, 25–40, <http://dx.doi.org/10.1038/s41418-018-0179-3>.
- Lasiene, J., Yamanaka, K., 2011. Glial cells in amyotrophic lateral sclerosis. *Neurol. Res. Int.* 2011, 718987, <http://dx.doi.org/10.1155/2011/718987>.
- Love, S., Miners, J.S., 2016. Cerebrovascular disease in ageing and Alzheimer's disease. *Acta Neuropathol.* 131, 645–658, <http://dx.doi.org/10.1007/s00401-015-1522-0>.
- Miyazaki, K., Ohta, Y., Nagai, M., Morimoto, N., Kurata, T., Takehisa, Y., Ikeda, Y., Matsuura, T., Abe, K., 2011. Disruption of neurovascular unit prior to motor neuron degeneration in amyotrophic lateral sclerosis. *J. Neurosci. Res.* 89, 718–728, <http://dx.doi.org/10.1002/jnr.22594>.
- Miyazaki, K., Masamoto, K., Morimoto, N., Kurata, T., Mimoto, T., Obata, T., Kanno, I., Abe, K., 2012. Early and progressive impairment of spinal blood flow-glucose metabolism coupling in motor neuron degeneration of ALS model mice. *J. Cereb. Blood Flow Metab.* 32, 456–467, <http://dx.doi.org/10.1038/jcbfm.2011.155>.
- Morrice, J.R., Gregory-Evans, C.Y., Shaw, C.A., 2017. Necroptosis in amyotrophic lateral sclerosis and other neurological disorders. *Biochim. Biophys. Acta - Mol. Basis Dis.* 1863, 347–353, <http://dx.doi.org/10.1016/j.bbdis.2016.11.025>.
- Nagara, Y., Tateishi, T., Yamasaki, R., Hayashi, S., Kawamura, M., Kikuchi, H., Iinuma, K.M., Tanaka, M., Iwaki, T., Matsushita, T., Ohyagi, Y., Kira, J., 2013. Impaired cytoplasmic-nuclear transport of hypoxia-inducible factor-1 α in amyotrophic lateral sclerosis. *Brain Pathol.* 23, 534–546, <http://dx.doi.org/10.1111/bpa.12040>.
- Niedzielska, E., Smaga, I., Gawlik, M., Moniczewski, A., Stankowicz, P., Pera, J., Filip, M., 2016. Oxidative stress in neurodegenerative diseases. *Mol. Neurobiol.* 53, 4094–4125, <http://dx.doi.org/10.1007/s12035-015-9337-5>.
- Nielsen, R.B., Egefjord, L., Angleys, H., Mouridsen, K., Gejl, M., Møller, A., Brock, B., Brændgaard, H., Gottrup, H., Rungby, J., Eskildsen, S.F., Østergaard, L., 2017. Capillary dysfunction is associated with symptom severity and neurodegeneration in Alzheimer's disease. *Alzheimer's Dement.* 13, 1143–1153, <http://dx.doi.org/10.1016/j.jalz.2017.02.007>.
- Nortley, R., Korte, N., Izquierdo, P., Hirunpattarasilp, C., Mishra, A., Jaunmuktane, Z., Kyrgyryi, V., Pfeiffer, T., Khennouf, L., Madry, C., Gong, H., Richard-Loendt, A., Huang, W., Saito, T., Saido, T.C., Brandner, S., Sethi, H., Attwell, D., 2019. Amyloid β oligomers constrict human capillaries in Alzheimer's disease via signaling to pericytes. *Science* (80-), 365, eaav9518, <http://dx.doi.org/10.1126/science.aav9518>.
- Oku, H., Ueda, Y., Iinuma, M., Ishiguro, K., 2005. Inhibitory effects of xanthenes from guttiferæ plants on PAF-induced hypotension in mice. *Planta Med.* 71, 90–92, <http://dx.doi.org/10.1055/s-2005-837760>.
- Philips, T., Rothstein, J.D., 2015. Rodent models of amyotrophic lateral sclerosis. In: *Current Protocols in Pharmacology*. John Wiley & Sons, Inc., Hoboken, NJ, USA, pp. 5.67.1–5.67.21, <http://dx.doi.org/10.1002/0471141755.ph0567s69>.
- Renton, A.E., Chiò, A., Traynor, B.J., 2014. State of play in amyotrophic lateral sclerosis genetics. *Nat. Neurosci.* 17, 17–23, <http://dx.doi.org/10.1038/nn.3584>.
- Rocha, L., Marston, A., Auxiliadora, M., Kaplan, C., Stoeckli-Evans, H., Thull, U., Testa, B., Hostettmann, K., 1994. An antifungal γ -pyrone and xanthenes with monoamine oxidase inhibitory activity from *Hypericum brasiliense*. *Phytochemistry* 36, 1381–1385, [http://dx.doi.org/10.1016/S0031-9422\(00\)89727-7](http://dx.doi.org/10.1016/S0031-9422(00)89727-7).
- Rosen, D.R., Siddique, T., Patterson, D., Figlewicz, D.A., Sapp, P., Hentati, A., Donaldson, D., Goto, J., O'Regan, J.P., Deng, H.-X., Rahmani, Z., Krizus, A., McKenna-Yasek, D., Cayabyab, A., Gaston, S.M., Berger, R., Tanzi, R.E., Halperin, J.J., Herzfeldt, B., Van den Bergh, R., Hung, W.-Y., Bird, T., Deng, G., Mulder, D.W., Smyth, C., Laing, N.G., Soriano, E., Pericak-Vance, M.A., Haines, J., Rouleau, G.A., Gusella, J.S., Horvitz, H.R., Brown, R.H., 1993. Mutations in Cu/Zn superoxide dismutase gene are associated with familial amyotrophic lateral sclerosis. *Nature* 362, 59–62, <http://dx.doi.org/10.1038/362059a0>.
- Sato, K., Morimoto, N., Kurata, T., Mimoto, T., Miyazaki, K., Ikeda, Y., Abe, K., 2012. Impaired response of hypoxic sensor protein HIF-1 α and its downstream proteins in the spinal motor neurons of ALS model mice. *Brain Res.* 1473, 55–62, <http://dx.doi.org/10.1016/j.brainres.2012.07.040>.
- Shimizu, S., Eguchi, Y., Kamiike, W., Itoh, Y., Hasegawa, J.I., Yamabe, K., Otsuki, Y., Matsuda, H., Tsujimoto, Y., 1996. Induction of apoptosis as well as necrosis by hypoxia and predominant prevention of apoptosis by Bcl-2 and Bcl-XL. *Cancer Res.* 56, 2161–2166.
- Tafari, M., Sansone, L., Limana, F., Arcangeli, T., De Santis, E., Polese, M., Fini, M., Russo, M.A., 2016. The interplay of reactive oxygen species, hypoxia, inflammation, and sirtuins in Cancer initiation and progression. *Oxid. Med. Cell. Longev.* 2016, 3907147, <http://dx.doi.org/10.1155/2016/3907147>.
- Taylor, J.P., Brown, R.H., Cleveland, D.W., 2016. Decoding ALS: from genes to mechanism. *Nature* 539, 197–206, <http://dx.doi.org/10.1038/nature20413>.
- Teh, S.S., Ee, G.C.L., Mah, S.H., Lim, Y.M., Ahmad, Z., 2013. Cytotoxicity and structure-activity relationships of xanthone derivatives from *Mesua beccariana*, *Mesua ferrea* and *Mesua congestiflora* towards nine human cancer cell lines. *Molecules* 18, 1985–1994, <http://dx.doi.org/10.3390/molecules18021985>.
- Thonhoff, J.R., Gao, J., Dunn, T.J., Ojeda, L., Wu, P., 2012. Mutant SOD1 microglia-generated nitrooxidative stress promotes toxicity to human fetal neural stem cell-derived motor neurons through direct damage and noxious interactions with astrocytes. *Am. J. Stem Cells* 1, 2–21.
- Uchida, Y., Ito, K., Ohtsuki, S., Kubo, Y., Suzuki, T., Terasaki, T., 2015. Major involvement of Na⁺-dependent multivitamin transporter (SLC5A6/SMVT) in uptake of biotin and pantothenic acid by human brain capillary endothelial cells. *J. Neurochem.* 134, 97–112, <http://dx.doi.org/10.1111/jnc.13092>.
- van Es, M.A., Hardiman, O., Chio, A., Al-Chalabi, A., Pasterkamp, R.J., Veldink, J.H., van den Berg, L.H., 2017v. Amyotrophic lateral sclerosis. *Lancet* (London, England) 390, 2084–2098, [http://dx.doi.org/10.1016/S0140-6736\(17\)31287-4](http://dx.doi.org/10.1016/S0140-6736(17)31287-4).
- Yi, B., Hu, L., Mei, W., Zhou, K., Wang, H., Luo, Y., Wei, X., Dai, H., 2011. Antioxidant phenolic compounds of cassava (*Manihot esculenta*) from Hainan. *Molecules* 16, 10157–10167, <http://dx.doi.org/10.3390/molecules161210157>.
- Zeisel, A., Hochgerner, H., Lönnerberg, P., Johnsson, A., Memic, F., van der Zwan, J., Häring, M., Braun, E., Börm, L.E., La Manno, G., Codeluppi, S., Furlan, A., Lee, K., Skene, N., Harris, K.D., Hjerling-Leffler, J., Arenas, E., Ernfors, P., Marklund, U., Linnarsson, S., 2018. Molecular architecture of the mouse nervous system. *Cell* 174, 999–1014, <http://dx.doi.org/10.1016/j.cell.2018.06.021>, e22.
- Zhigalova, N., Artemov, A., Mazur, A., Prokhortchouk, E., 2015. Transcriptome sequencing revealed differences in the response of renal cancer cells to hypoxia and CoCl₂ treatment. *F1000Research* 1518, 1–8, <http://dx.doi.org/10.12688/f1000research.7571.1>.
- Zlokovic, B.V., 2008. The blood-brain barrier in health and chronic neurodegenerative disorders. *Neuron* 57, 178–201, <http://dx.doi.org/10.1016/j.neuron.2008.01.003>.